from 4 to 5·5 dB in the same frequency range. This amplifier operates at a drain bias of 3·5 V and requires 20–25 mA of current.

Conclusion: InP has not been in widespread use for MMIC applications owing to the absence of a high-performance, general-purpose, three-terminal active device implementation on it. The present work shows that with the highly successful millimetre wave results recently obtained with GaInAs/AlInAs HEMTs lattice-matched to InP, this material becomes a viable alternative to GaAs as a substrate material for MMICs, and paves the way towards more advanced integrated optoelectronic circuits.

The processing steps involved in the fabrication of MMICs on InP are very similar to those used with GaAs. One exception is the RIE via hole process which may yield nonvolatile indium byproducts and needs to be optimised separately for InP. This problem was not encountered in the present work due to the use of CPW transmission lines.

M. RIAZIAT
Y. C. PAO
C. NISHIMOTO
G. ZDASIUK
S. BANDY
S. L. WENG

Varian Research Center
611 Hansen Way, Palo Alto, CA 94303, USA

4th July 1989

References

1 MAYCOCK, P. D.: 'Thermal conductivity of silicon, germanium, III-V compounds and III-V alloys', *Solid-State Electron.*, 1987, **10**, pp. 161–168
2 RIDLEY, B. K.: 'Anatomy of the transferred electron effect in III-V semiconductors', *J. Appl. Phys.*, 1977, **48**, (2)
3 ARMAND, M., CHEVRIER, J., and LINH, N. T.: 'Microwave power amplification with InP FETs', *Electron. Lett.*, 1980, **16**, pp. 906–907
4 BANDY, S., NISHIMOTO, C., HYDER, S., and HOOPER, C.: 'Saturation velocity determination for InGaAs field effect transistors', *Appl. Phys. Lett.*, 1981, **38**, (10)
5 SEO, K. S., BHATTACHARYA, P. K., and NASHIMOTO, Y.: 'An InGaAs–InAlAs single quantum well field effect transistor', *Electron Device Lett.*, 1985, **EDL-6**, (12)
6 HO, P., CHAO, P. C., DUH, K. H., JABRA, A. A., BALLINGALL, J. M., and SMITH, P. M.: 'Extremely high gain, low noise InAlAs/InGaAs HEMTs grown by molecular beam epitaxy'. IEDM Technical Digest, Dec. 1988
7 YARIV, A.: 'Optical electronics' (HRW, New York, 1985)
8 RIAZIAT, M., PAR, E., ZDASIUK, G., BANDY, S., and GLENN, M.: 'Monolithic millimeter wave CPW circuits'. 1989 IEEE MTT-S International Microwave Symposium Digest, June 1989

EFFECT OF COCHANNEL INTERFERENCE ON HANDOVER IN MICROCELLULAR MOBILE RADIO

Indexing terms: Radiowave propagation, Mobile radio systems, Interference, Digital communication systems

The effect of cochannel interference on a fast handover algorithm for microcellular mobile radio systems is described. The presence of cochannel interference had only a marginal effect on the handover point when the microcell base stations were spaced by 300 m. Increasing the mobile speed increased the effective cell length.

It is vital in digital microcellular mobile radio systems to deploy rapid handover procedures that impose a minimum of loading on the network as the mobile roams between microcells. One approach[1] that satisfies these requirements is to connect the microcellular base stations (BSs) and the mobile switching centre (MSC) to a ring optical local area network (LAN). For narrowband time division multiple access (NB-TDMA) mobile communications the data is essentially in a packet form that is suitable for the LAN. Handover from one BS to another involves addressing the packets for the mobile station (MS) to the new BS, with suitable instructions for the MS to resynthesise its frequency. The handover procedure as far as the LAN is concerned is essentially readdressing packets. There is no network loading beyond the LAN until the MS roams out of the area controlled by the MSC, when information data must be routed from the ISDN/PSTN to the new MSC.[1]

There are numerous approaches to handover, but the one we favour is based on the bit error rate (BER) as this is a good indicator of speech quality. Further, the decision to handover is made by continuously monitoring the BER of the speech communications in progress. Suppose the communications are between BS_A and an MS. The speech data is Reed–Solomon-coded by an RS(n, k) code, where k and n are the number of data symbols before and after coding, respectively. The speech-coded data are transmitted by the MS, and BS_A notes the symbol error rate (SER) (from the RS decoder's error locator polynomial) during every codeword, even though the errors may be corrected. If the RS decoder is overloaded, it deems that $t = (n - k)/2$ symbol errors occurred. There will in fact be more than t errors, although the use of systematic RS codes prevents all the data being scrambled as a consequence of code overload. A running average symbol error rate R_A over M_P code words is performed. Suppose another BS, BS_B, is sufficiently close to the MS to monitor the MS's transmissions to BS_A. BS_B computes a running symbol error rate R_B for the MS to BS_A transmissions. The R_A and R_B values are placed in packets and conveyed to the MSC via the LAN. The MSC computes R_A/R_B, and if this ratio exceeds a threshold K, a parameter P_j is set to unity. If not, P_j is made zero. As the statuses of the most recently received packets are more significant in determining handover, a summation of $P_j W_j$ is made over M_W packets, where $W_j = M_W + 1 - j$ ($j = 1, 2, \ldots, M_W$). Should $P_j W_j$ ($j = 1, 2, \ldots, M_W$) exceed a threshold A, and the current $R_A > E$, where A and E are system parameters, handover of the MS communications to BS_B ensues.

In our simulations, telephonic speech at 8 ksamples/s was sub-band coded (SBC) at 16 kbit/s, and a systematic RS(56, 28) codec was used with 8 bits per symbol. The coded data modulated a binary shift keying (BPSK) modulator to form the transmitted signal from the MS, which was assumed to be travelling at a constant speed of 30 mph (unless otherwise stated) along a straight road. The choice of the radio channel between the BS and the MS was based on propagation experiments made in microcellular environments in central London and on highways in southern England, where it was shown[2] that, in general, an inverse-fourth-power path loss law prevailed. Accordingly we have used this law in our simulations. The fast fading in microcells is Rician, although near Gaussian and Rayleigh PDFs of received signal envelopes have also been observed.[3] We elected to use a Rayleigh PDF as it provided worst-case fadings conditions. Bandlimited white Gaussian noise with a mean of −120 dBm was present at the input of the coherent binary phase shift keying (BPSK) demodulator. After BPSK demodulation at the BS, the data was RS(56, 28)-decoded, followed by SBC decoding to recover the speech signal. The SER_A was computed as described above.

The adjacent BS, BS_B, monitored the MS's transmissions via an independent Rayleigh fading/inverse fourth-power law channel, and computed SER_B. The SER_A and SER_B data was conveyed via an optical packet LAN to the MSC and the handover calculations performed. Handover was then enacted according to the algorithm, whose parameters were $M_p = 50$, $K = 5$, $M_W = 10$, $E = 10^{-2}$ and $A = 0{\cdot}65$.

The MS was assumed to be travelling in a 2-cell cluster. The BSs were spaced by a distance L, giving a cochannel distance in the vicinity of handover of approximately $1{\cdot}5L$. The transmitter power was adjusted so that in the absence of cochannel interference handover occurred when the BER after channel decoding became significantly higher than 10^{-3}. Thus in the simulations the MS and BS_A were involved in a two-way communications, BS_B was in a listening mode monitoring the MS reception, while BS_I transmitted at the same power level and on the same carrier frequency over an independent fading channel, resulting in cochannel interference.

Fig. 1 shows the variation of the BER with distance along the road as the MS moved away from BS_A in the presence and in the absence of cochannel interference. The BS separation L was 300 m and the BER was formulated by averaging over a duration equivalent to 4 RS codewords. The decoded BER was generally zero owing to the effectiveness of the RS channel coding until the MS was close to the handover point at 162 m from the BS_A. However, there were a few instances over this distance when the RS codec was overloaded yielding error bursts. When the vehicular speed was increased to 60 mile/h the handover position was at 179 m from BS_A.

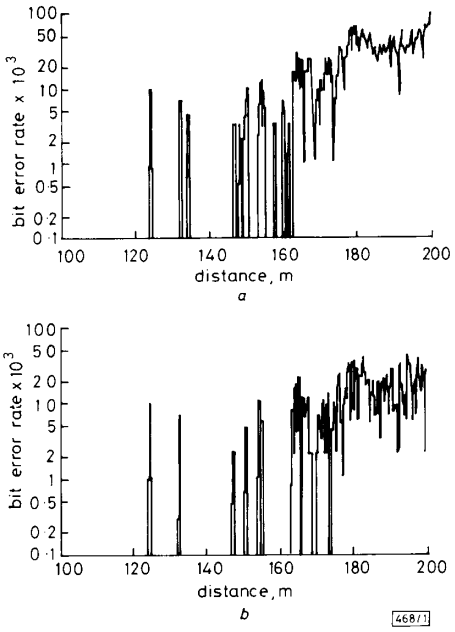

Fig. 1 *BER distance profile (a) in presence and (b) in absence of cochannel interference*

Mobile speed = 30 mile/h, L = 300 m

Returning to a vehicular speed of 30 mph, and introducing cochannel interference, we found that the interference had only a marginal effect on the BER profile, except near the handover region. The handover location was 158 m from BS_A. (We noted that when the radiated power from BS_I was three times greater than that from BS_A the handover distance decreased to 145 m).

Fig. 2 shows the decoded BER profile when cochannel interference was present and communications with the mobile station were with BS_A, and for comparison purposes the absence of cochannel interference when the communications were switched to BS_B. Only one handover occurred, and that was at 158 m from BS_A. The averaging of the decoded BER was again done over 4 RS code blocks. The decoded BER performance can be enhanced by altering the handover parameters, when the number of handovers will increase.[1] We increased L to 500 m, raised the transmitted powers appropriately and observed a similar BER performance, with the handover at 264 m from BS_A. As Rician fades are less deep than Rayleigh ones, we confidently predict the effect of cochannel interference on the handover location will be even less influential than shown here.

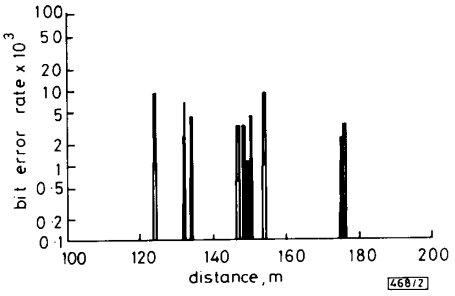

Fig. 2 *BER distance profile*

Cochannel interference was present when communications were via BS_A, while after handover to BS_B cochannel interference was absent. Mobile speed = 30 mile/h, L = 300 m

R. STEELE
D. TWELVES
L. HANZO

Department of Electronics & Computer Science
University of Southampton
Southampton SO9 5NH, United Kingdom

13th July 1989

References

1 STEELE, R.: 'The cellular environment of the light-weight hand-held portable', *IEEE Commun. Mag.*, 1989, **27**, (7), pp. 20–29
2 CHIA, S. T. S., STEELE, R., GREEN, E., and BARAN, A.: 'Propagation and bit error ratio measurements for a microcellular system', *J. IERE*, 1987, **57**, (6) (Supplement), pp. S255–S266
3 GREEN, E.: 'Co-channel and BER measurements taken in a microcellular environment'. IEE Colloquium, London, Digest No. 1989/29, 22 Feb 1989, pp. 6/1–6/8

LOW-LOSS STRAIGHT AND CURVED RIDGE WAVEGUIDES IN LPE-GROWN GaInAsP

Indexing terms: Integrated optics, Optical waveguides, Optical communications, Optoelectronics

Loss measurements on ridge waveguides in LPE-grown GaInAsP at a wavelength of 1·3 μm are presented. An attenuation of 4·5 dB/cm has been obtained for straight waveguides, and for curved waveguides an excess loss as low as 0·7 dB was found for a 20·8° S-bend with a radius of 300 μm (≈1·5 dB/90°).

Introduction: The development of fibre-based telecommunications demands cheap, reliable and small optoelectronic integrated circuits (OEICs). These circuits will operate at a wavelength of 1·2 μm or 1·55 μm. The only material suitable for the integration of both passive and active components on one wafer is GaInAsP lattice matched to InP.

Low-loss straight and curved waveguides are essential to achieve the required optoelectronics circuits. Optical losses in straight waveguides are due to absorption and to scattering by interface roughness, and can therefore be reduced by lowering the background doping level by using small refractive index contrasts and reactive ion etching (RIE) to produce smooth edges.[1] The losses in curved waveguides are due to radiation and to transitions between straight and curved sections (conversion losses). Radiation losses decrease with increasing lateral refractive index contrast. Conversion losses are caused by mode mismatch and can be reduced by offsetting the curved waveguide with respect to the straight waveguide. It is obvious that, concerning the refractive index contrast, there is a trade-off between scattering losses in straight waveguides and radiation losses in curved waveguides.

To our knowledge no experimental results on bending losses have been published so far for InP-based curved waveguides. Austin and Flavin, however, found[2] 1 dB/90° for GaAs/AlGaAs ridge waveguides with a radius of curvature of 300 μm at a wavelength of 1·15 μm. In this letter we report on bending losses for curved ridge waveguides in GaInAsP on InP, etched by RIE. Theoretical calculations have been done to find the optimal offsets and to verify the experimental results. The bending losses have been determined for both polarisations.

Experiments: A number of straight waveguides together with four different S-bends have been fabricated in a double hetero (DH) structure with a width of 1·9 μm and a ridge height of